


voyAGEr: first steps

The web application

voyAGEr is freely available at

<https://compbio.imm.medicina.ulisboa.pt/voyAGEr>

voyAGEr is composed of four main sections (the tabs in the navigation bar at the top):

- **Home** (depicted by the home icon  and no literal titling): to visually explain the used method and its associated findings featured in the application.
- **Gene**: to lead a gene-centric investigation, namely to assess how the expression of a specific gene changes with age and sex in a specific tissue.
- **Tissue**: to analyse how tissue-specific transcriptomes change with age and sex.
- **Module**: to further examine sets of co-expressed genes whose expression is altered with age namely through their enrichment in specific cell types, biological pathways and association with diseases.

voyAGEr leverages RNA-seq datasets from the GTEx project (Lonsdale et al., 2013), encompassing tissue samples from hundreds of donors aged from 20 to 70 years.

Senescence-associated genes

Cellular senescence is a stress-induced cell cycle arrest limiting proliferation of potentially oncogenic cells but progressively creating an inflammatory environment in tissues as they age and therefore an example of a process whose molecular mechanisms are of particular interest to ageing researchers (Gorgoulis et al., 2019; Van Deursen, 2014).

Senescence markers, such as *CDKN2A*, encoding cell cycle regulatory protein p16^{INK4A} that accumulates in senescent cells (Erickson et al., 1998; Gil & Peters, 2006), can thus be studied as putative markers of ageing of certain tissues.

CDKN2A expression profile

To examine *CDKN2A* expression changes across age: 1- Go to the **Gene section**

2- Type *CDKN2A* in the **Gene field**

The application then features:

- i- in the **Profile sub-tab**, a heatmap of tissue-specific *CDKN2A* scaled expression (Z-scores) across age, for all tissues (**Figure 1**).
- ii- in the **Alteration sub-tab**, a heatmap of significance of tissue-specific *CDKN2A* expression age-related alterations due to Age, Sex or Age&Sex (depending on the user's choice – **Alterations associated with field** on the left), for all tissues (**Figure 2**).

This section might take a bit longer to load.

Note that gene names in vyAGER are HGNC (HUGO Gene Nomenclature Committee) symbols. For each gene, the respective NCBI and GeneCards webpages can be accessed by clicking on their logos next to its name on plot's title.

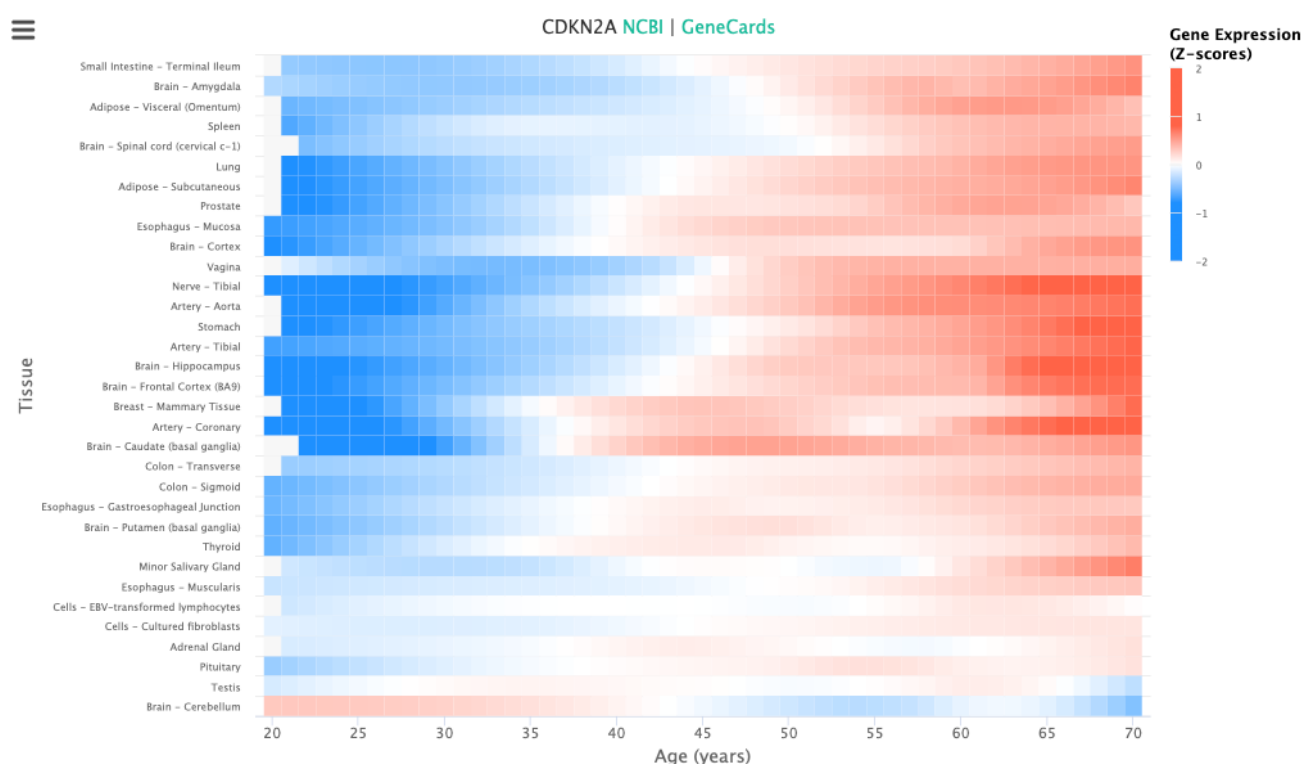


Figure 1 – Heatmap of tissue-specific *CDKN2A* expression over age.

- 3- Go to the **Alteration sub-tab** to check the significance of *CDKN2A* expression alterations across tissues and age (leave the default parameters, *All tissues* and *Age*, in the **Tissue** and **Alterations associated with fields**, respectively). A heatmap like that of **Figure 2** is featured.

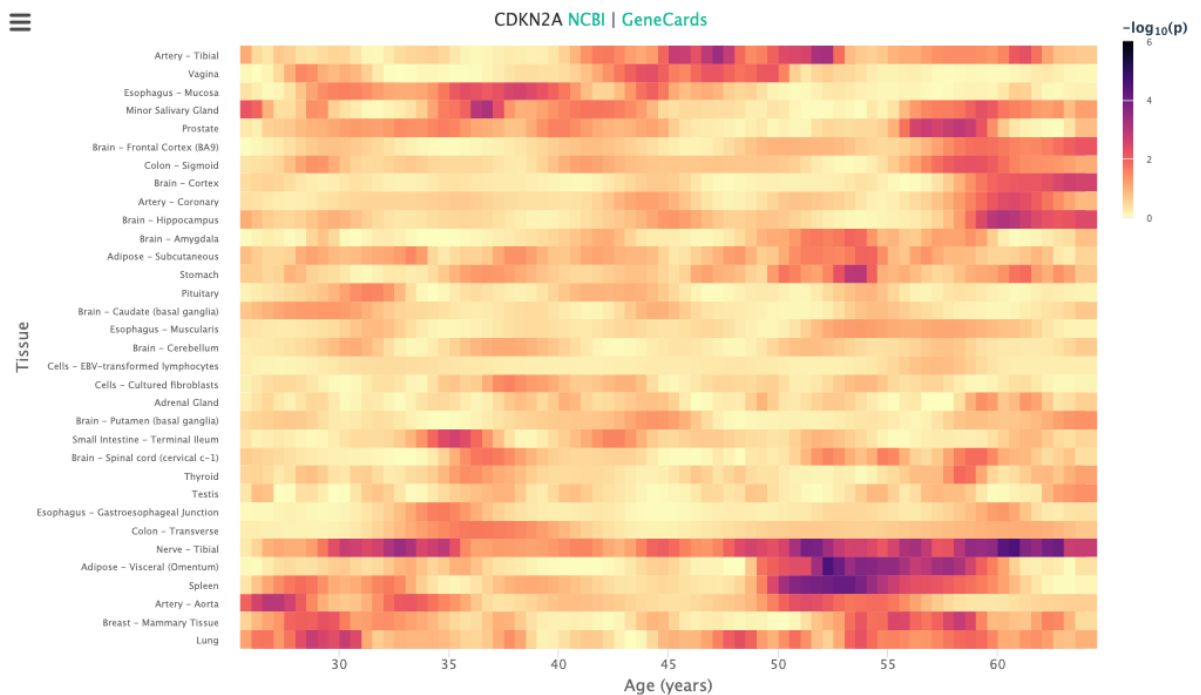


Figure 2 – Heatmap of significance of tissue-specific Age-associated *CDKN2A* expression alterations over age.

- 4- Enter/select *Lung* in the **Tissue** field to investigate *CDKN2A* expression changes in that specific tissue.

Plots of *CDKN2A* expression (top panel, identical to that in the *Profile* sub-tab) and the significance of its alterations over age (bottom panel) are then featured (**Figure 3**). Significant *CDKN2A* expression increases are observed in the late forties and early sixties.

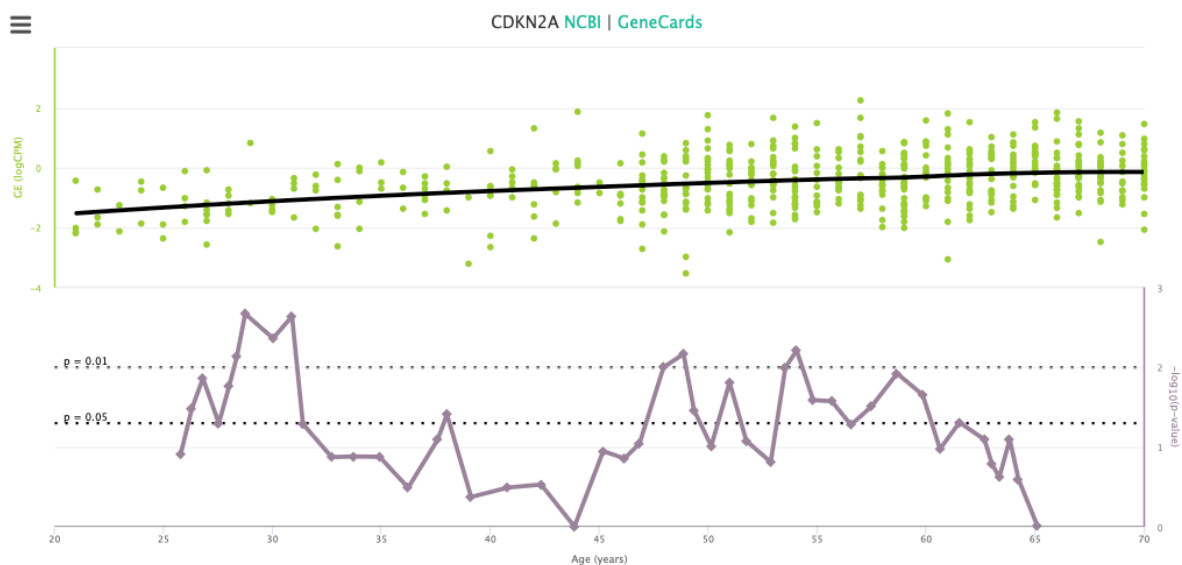


Figure 3 – *CDKN2A* expression in the lung (top panel) and significance of its alterations (bottom panel) over age.

- 5- Go to the **Profile sub-tab**. voyAGER can also associate *CDKN2A* expression in the lung with the donors' sex and medical history. These clinical data are displayed in a table below the expression profile's scatter plot.

GTEx transcriptomic data are from "healthy" tissue samples from donors that had, nonetheless, reported medical conditions (Lonsdale et al., 2013).

- i- Click on Sex in the **Coloured by** field, leaving *All* in the **Shaped by** field.

CDKN2A lung expression progression with age appears to be influenced by the donors' sex, particularly in the mid-thirties (**Figure 4**). This observation can be statistically tested in the **Alteration sub-tab** by clicking on Sex in the **Alterations associated with** field.

- ii- Back in the *Profile* sub-tab, click on *All* in the **Coloured by** field and on *Condition* in the **Shaped by** field. Enter/select *MHCOPD* in the **Select** field.

The *CDKN2A* lung expression profile is herein associated with medical conditions (positive if the donor suffered from the condition, negative if not and unknown if the association is uncharted). Moreover, the median gene expression values for positive and negative conditions are displayed. The significance of Kruskal-Wallis tests for the difference in gene expression medians between positive and negative donors is used to rank conditions. In this case, the condition selected (Chronic Respiratory Disease) is amongst those displaying a significant difference in median (adjusted p-value below 0.05). On the scatter plot with *CDKN2A* lung expression over age, the curves fitted independently for positive and negative conditions show that such difference in gene expression occurs mostly after the age of 50 (**Figure 5**).

Limitations: In the GTEx dataset, there are conditions for which very few donors are positive and others for which very few donors have their condition state annotated. The significance of the Kruskal-Wallis tests must therefore be regarded with caution and as providing limited information. In this case, for example, even though significant differences in median were found for the History of Non Metastatic Cancer and Cocaine Use in 5 years, the low number of positive samples and their concentration in limited age ranges hamper any solid conclusion.

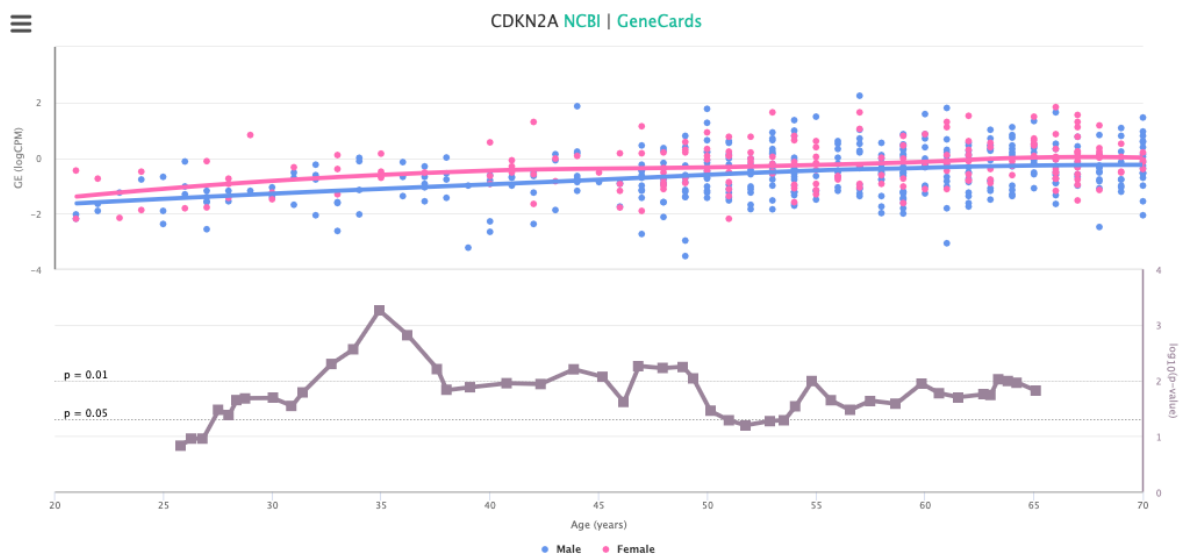


Figure 4 – *CDKN2A* expression in the lung, discriminated between donors sex (female in pink, male in blue) over age.

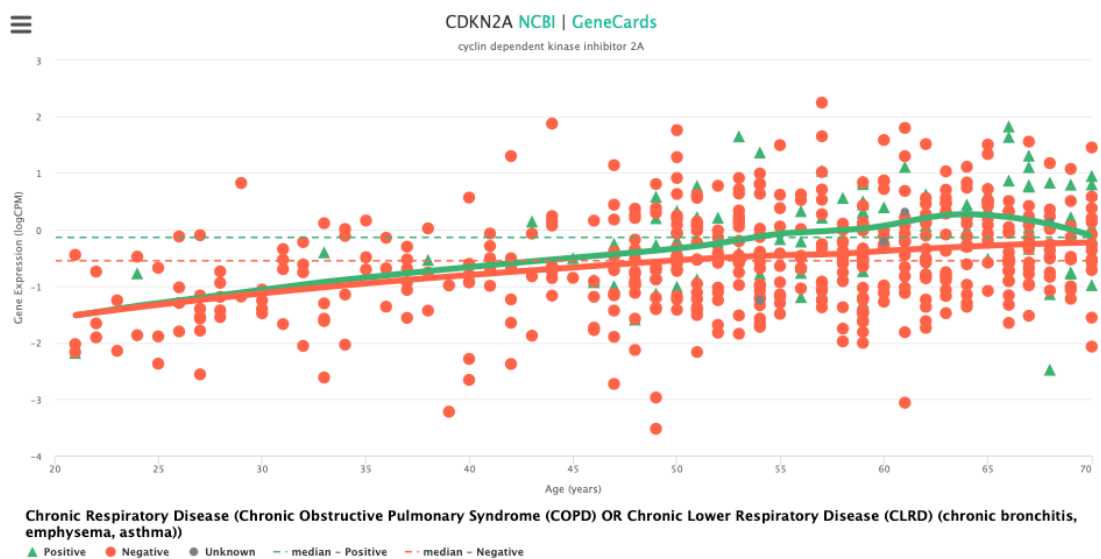


Figure 5 – *CDKN2A* expression in the lung, discriminated between donors with (green) and without (orange) abnormal white blood count, over age.

Transcriptional changes in the Transverse colon

1- Go to the **Tissue** section.

The landscape of Age-, Sex- and Age&Sex-associated global gene expression alterations along age for all tissues can be profiled using the significance of proportions of differentially expressed genes. Three periods stand out with significant transcriptional changes associated with Age (keeping the default *All tissues* in the **Tissue** field and Age in the **Alterations associated with field**), after 55 years old (**Figure 6**). Moreover, most of the significant transcriptional differences between sexes appear to occur in the fifth and sixth decades of life (*All tissues* in the **Tissue** field and Sex in the **Alterations associated with field**) (**Figure 7**).

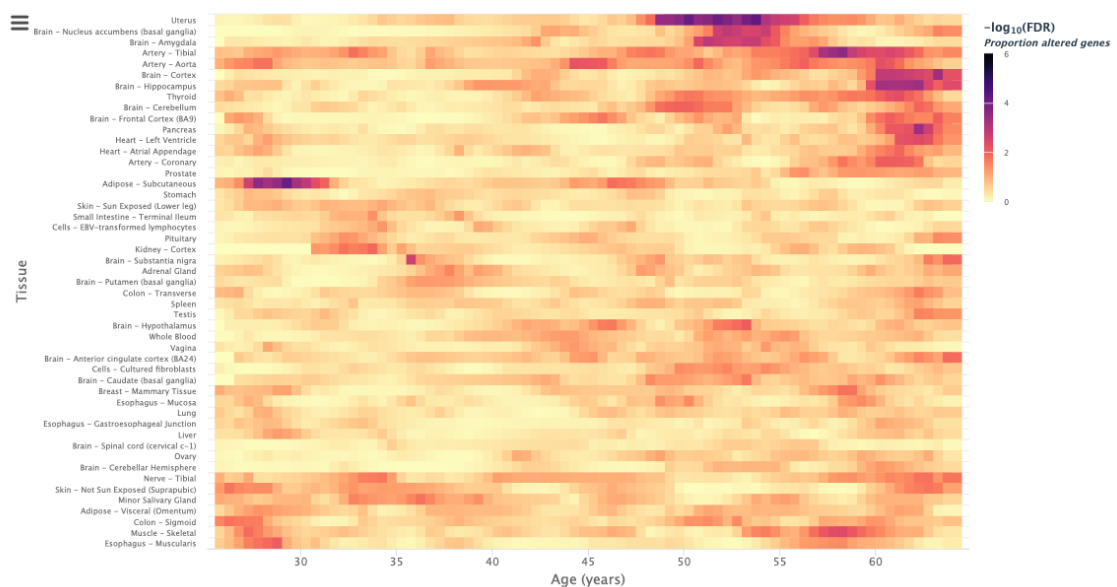


Figure 6 – Heatmap of significance of tissue-specific Age-associated global gene expression alterations over age.

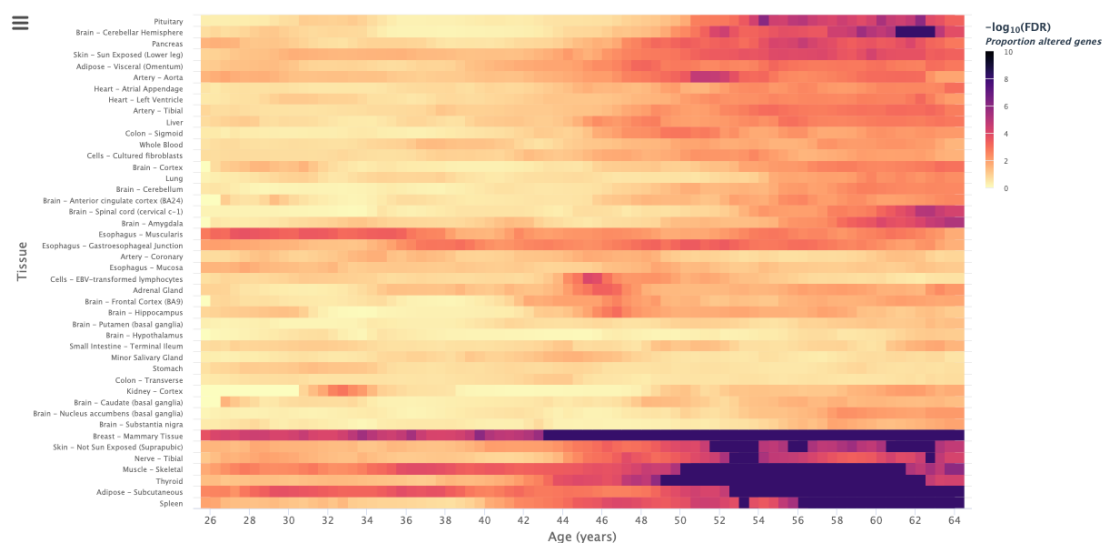


Figure 7 – Heatmap of significance of tissue-specific Sex-associated global gene expression alterations over age.

- 2- Enter *Adipose – Subcutaneous* in the **Tissue** field and click on *Age* in the **Alterations associated with field**.

The progression of the percentage of Age-associated altered genes over age is now featured (**Figure 8**). The statistical significance of each proportion is also illustrated with a colour scale. Two periods of significant transcriptional changes appear to occur, at late 20's (13.6% altered genes) and late 40's (4.7% altered genes).

- 3- Click on the dot at 29.57 years old (hovering over each point in the plot will show its details).

The list of differentially expressed genes, ordered by their significance, appears on the left (**Figure 8**).



Figure 8 – Progression of the percentage of Age-associated altered genes overage in Adipose - Subcutaneous. For each age, the list of the most altered genes can be obtained by clicking on the respective dot.

- 4- Click on the *LMO3* row in the table.
Plots of *LMO3* expression and the significance of its alterations over age (like in Figure 3) appear.
- 5- Browse the expression alterations' significance over age of the most altered genes by selecting them in the table.
Some (e.g., *PRELID1*, *RUNX1T1*, *FGFRL1*) have their expression significantly modified only in the aforementioned first peak at around 28 years old.
- 6- Click on the dot at 46.43 y.o. and similarly browse the expression alterations' significance of the most differentially expressed genes at this age.
Some (e.g. *MT-CYB*, *MT-ND4*, *MT-ATP6*, *MT-ND2*) have their expression significantly altered only in this second peak.

Different sets of genes may drive the different age periods of major transcriptional changes, which begs assessing if they reflect the activation of distinct biological processes. For this purpose, the user can profile the biological functions of the genes underlying each peak of transcriptomic changes by assessing their enrichment in manually curated pathways from the Reactome database (Croft et al., 2014) or in user-provided gene sets.

7- Go to the **Enrichment sub-tab**.

A heatmap showing the normalised enrichment score (NES) of Reactome pathways (columns) along age (row) is displayed (**Figure 9**). The percentage of altered genes over age can be found on the right side of the heatmap. Reactome pathways are gathered in families of biological functions, based on shared genes, that can be found at the top of the heatmap.

Note that, for visualisation ease, only the most significantly associated pathways are featured.

The user can click on *Select:* in the **Pathway field** to examine results for a given Reactome pathway.

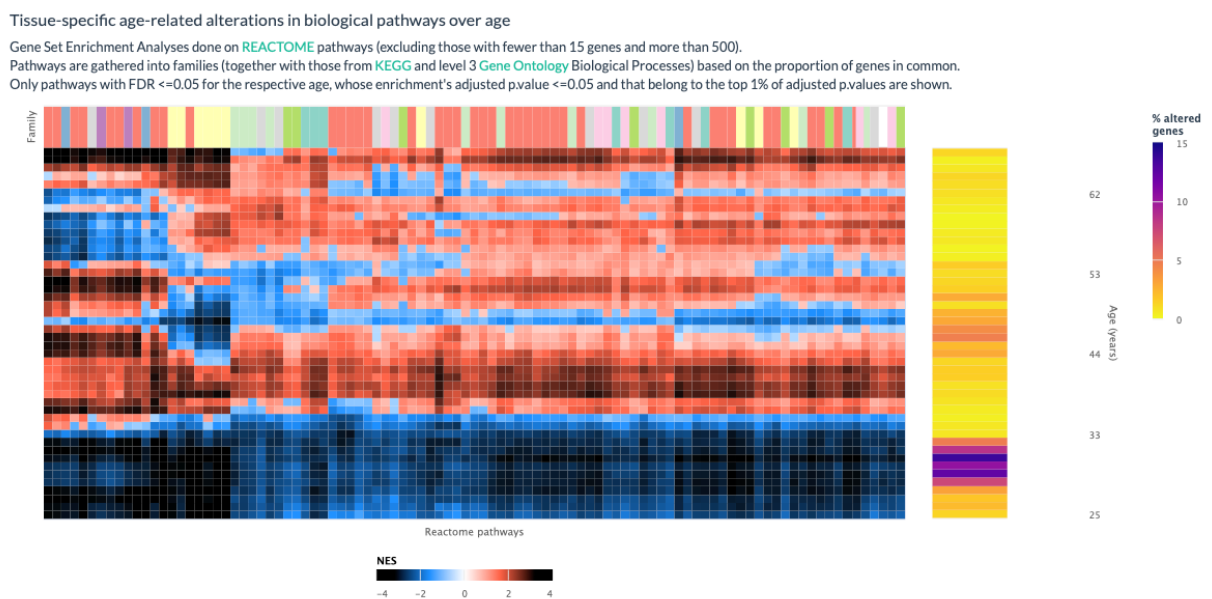


Figure 9 – Heatmap of significance of tissue-specific Age-associated global gene expression alterations over age.

8- Below the heatmap, click on the red family (family 3) in the **Families of pathways section**.

A word cloud provides a glimpse into the family's biological functions.

By clicking on the **Pathways sub-tab** in the **Families of pathways section**, the user has access to the list of specific pathways from the Reactome, Gene

Ontology (Gene Ontology Consortium, 2004) and KEGG (Kanehisa, 2000) databases that are associated with the family.

- 9- Click on *User-specified* in the **Geneset** field on the left.

Let's examine the enrichment of the three peaks of transcriptional changes in senescent-associated genes.

- 10- Enter the 230 senescent-associated genes (retrieved from Senequest (Gorgoulis et al., 2019) whose link with senescence is supported by at least 4 sources) from this document's appendix in the **List of genes** field, leave a Significance threshold p-value of 0.05 and **Run**.

Although we have two peaks, if you hover over the tip you'll notice neither of them are significantly enriched in senescence-associated genes (**Figure 10**).

Gene symbols can be in upper or lower case but must still follow the HGNC naming. If a gene symbol is not recognised as such, the gene is not included in the analysis.

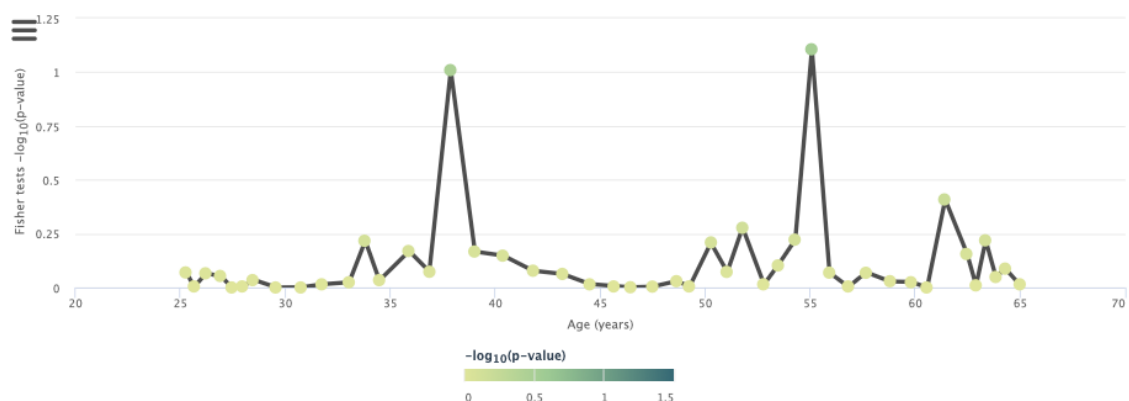


Figure 10 – Enrichment of altered genes amongst senescent-associated genes over age (non significant).

Modules of co-expressed genes

Genes with highly correlated expression are likely to be coregulated and share biological functions or associations with phenotypical or pathological traits (van Dam et al., 2017). Clusters of these genes, called modules, are identified in 4 tissues using voyAGER and their enrichment in cell types, Reactome pathways, and disease markers can be analysed.

- 1- Go to the **Results sub-section** of the **Module section**.

The **About sub-section** graphically summarises the methods employed to obtain the modules.

Each module is made of a set of genes and characterised by an eigengene representing their average expression profile.

Modules' eigengene expression and enrichment in Reactome pathways, cell types, and disease markers can be respectively found in the 4 sub-tabs: Expression, Cell types, Pathways, Diseases.

- 2- Choose *Brain - Cortex* in the **Tissue field**.

6 modules were identified in this tissue. Each module is named based on the colour used to depict it.

- 3- Go to the **Cell types sub-tab**.

For each tissue, cell types and their markers were retrieved from the literature and then differ from a paper to another. Regarding the Brain - Cortex analysis, we can see that the annotation of cell types from Fan (Fan et al., 2018) is more comprehensive than Descartes (Cao et al., 2020).

Select the Descartes signature. At least four of the 5 modules appear to be particularly enriched for certain cell types markers (**Figure 11**): the yellow module for Microglia, turquoise for Endothelial cells, brown for oligodendrocytes, and blue for astrocytes.

- 4- Change the source of cell type markers by clicking on a different row in the table on the left.

For both sources, the cell types enriched in the 4 modules match.

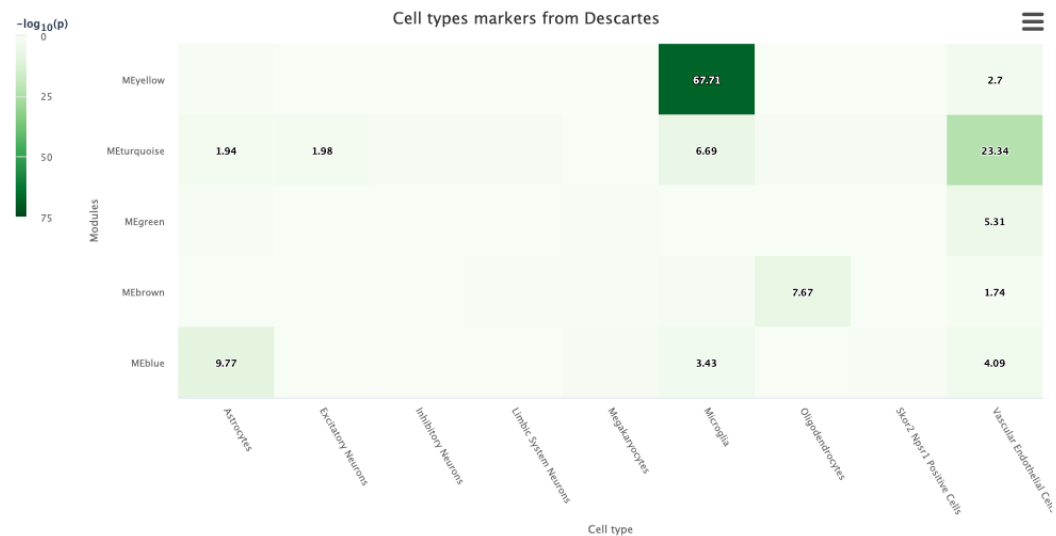


Figure 11 – Enrichment of modules of co-expressed genes identified the brain cortex in cell types markers from Cao et al. (2020)

5- Choose *MEyellow* in the **Module** field.

The four layers of information captured in the four Module sub-tabs are now specifically displayed for the chosen module. Besides, the module's 121 genes are identified on the left. The expression of the module's eigengene appears to be roughly steady throughout life (**Figure 12**).

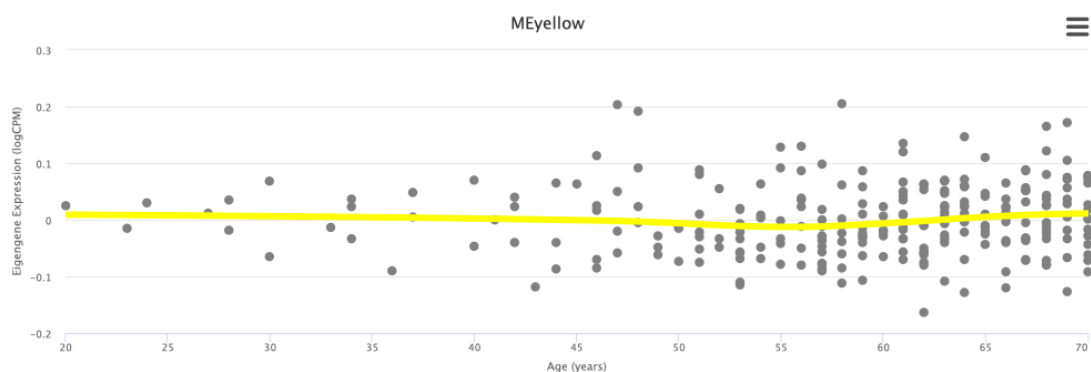


Figure 12 – Yellow module (associated with microglia) eigengene expression in the brain cortex over age.

6- Click on Sex in the **Colored by** field.

The module's eigengene expression does not seem to indicate that there are substantial differences in the yellow module over age, possibly suggesting that both male and females have a comparable proportion of microglia in the brain cortex (**Figure 13**).

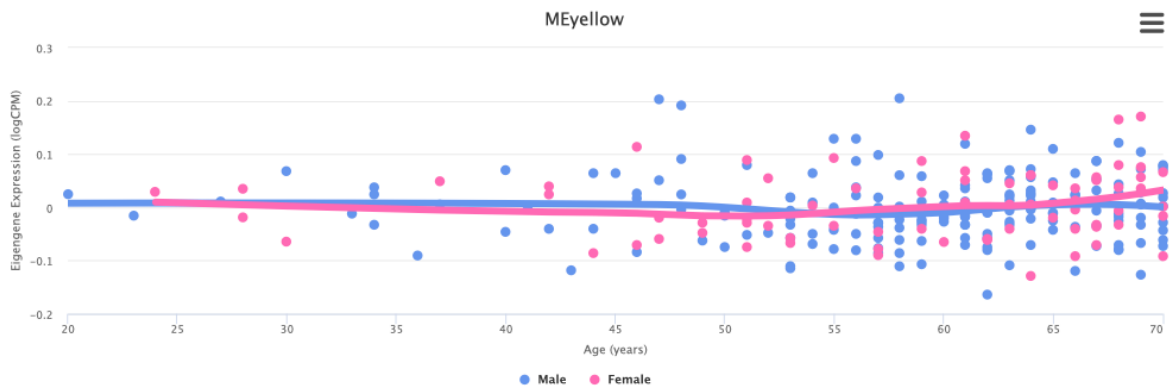


Figure 13 – Yellow module eigengene expression in the brain cortex, discriminated between sexes, over age.

- 7- Click on *All* in the **Colored by** field and on *Condition* in the **Shaped by** field. Choose *Cerebrovascular Disease* as condition. Eigengene expression appears to be slightly higher in positive when comparing to negative conditions, suggesting a role of microglia in these conditions (**Figure 14**), in accordance with what was already described in the literature (Dong et al. 2021).

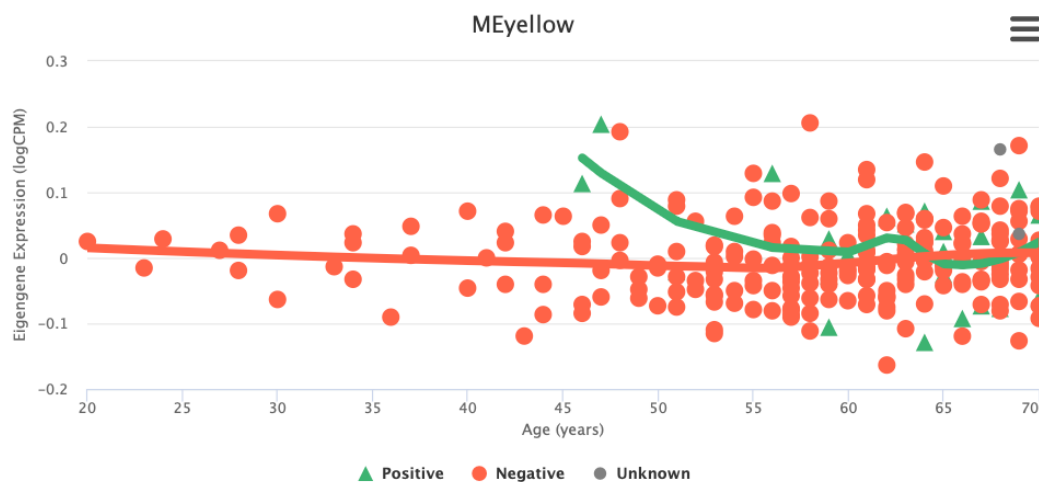


Figure 14 – Yellow module eigengene expression in the brain cortex, discriminated by the donors' "Cerebrovascular Disease" history, over age.

- 8- Explore the **Pathways** and the **Diseases-DisGeNET** sub-tabs.
As expected, the module is associated with immune-related Reactome pathways and diseases (e.g. rheumatoid arthritis).

References

- Croft, D., Mundo, A. F., Haw, R., Milacic, M., Weiser, J., Wu, G., Caudy, M., Garapati, P., Gillespie, M., Kamdar, M. R., Jassal, B., Jupe, S., Matthews, L., May, B., Palatnik, S., Rothfels, K., Shamovsky, V., Song, H., Williams, M., ... D'Eustachio, P. (2014). The Reactome pathway knowledgebase. *Nucleic Acids Research*, 42(D1), D472–D477. <https://doi.org/10.1093/nar/gkt1102>
- Cao, J., O'Day, D. R., Pliner, H. A., Kingsley, P. D., Deng, M., Daza, R. M., ... & Shendure, J. (2020). A human cell atlas of fetal gene expression. *Science*, 370(6518), eaba7721.
- Dong, R., Huang, R., Wang, J., Liu, H., & Xu, Z. (2021). Effects of microglial activation and polarization on brain injury after stroke. *Frontiers in neurology*, 12, 620948.
- Erickson, S., Sangfelt, O., Heyman, M., Castro, J., Einhorn, S., & Grandér, D. (1998). Involvement of the Ink4 proteins p16 and p15 in T-lymphocyte senescence. *Oncogene*, 17(5), 595–602. <https://doi.org/10.1038/sj.onc.1201965>
- Fan, X., Dong, J., Zhong, S., Wei, Y., Wu, Q., Yan, L., ... & Tang, F. (2018). Spatial transcriptomic survey of human embryonic cerebral cortex by single-cell RNA-seq analysis. *Cell research*, 28(7), 730–745.
- Gene Ontology Consortium. (2004). The Gene Ontology (GO) database and informatics resource. *Nucleic Acids Research*, 32(90001), 258D – 261. <https://doi.org/10.1093/nar/gkh036>
- Gil, J., & Peters, G. (2006). Regulation of the INK4b–ARF–INK4a tumour suppressor locus: all for one or one for all. *Nature Reviews Molecular Cell Biology*, 7(9), 667–677. <https://doi.org/10.1038/nrm1987>
- Gorgoulis, V., Adams, P. D., Alimonti, A., Bennett, D. C., Bischof, O., Bishop, C., Campisi, J., Collado, M., Evangelou, K., Ferbeyre, G., Gil, J., Hara, E., Krizhanovsky, V., Jurk, D., Maier, A. B., Narita, M., Niedernhofer, L., Passos, J. F., Robbins, P. D., ... Demaria, M. (2019). Cellular Senescence: Defining a Path Forward. *Cell*, 179(4), 813–827. <https://doi.org/10.1016/j.cell.2019.10.005>
- He, S., Wang, L.-H., Liu, Y., Li, Y.-Q., Chen, H.-T., Xu, J.-H., Peng, W., Lin, G.-W., Wei, P.-P., Li, B., Xia, X., Wang, D., Bei, J.-X., He, X., & Guo, Z. (2020). Single-cell transcriptome profiling of an adult human cell atlas of 15 major organs. *Genome Biology*, 21(1), 294. <https://doi.org/10.1186/s13059-020-02210-0>
- Kanehisa, M. (2000). KEGG: Kyoto Encyclopedia of Genes and Genomes. *Nucleic Acids Research*, 28(1), 27–30. <https://doi.org/10.1093/nar/28.1.27>
- Lonsdale, J., Thomas, J., Salvatore, M., Phillips, R., Lo, E., Shad, S., Hasz, R., Walters, G., Garcia, F., Young, N., Foster, B., Moser, M., Karasik, E., Gillard, B., Ramsey, K., Sullivan, S., Bridge, J., Magazine, H., Syron, J., ... Moore, H. F. (2013). The Genotype-Tissue Expression (GTEx) project. *Nature Genetics*, 45(6), 580–585. <https://doi.org/10.1038/ng.2653>
- Skelly, D. A., Squiers, G. T., McLellan, M. A., Bolisetty, M. T., Robson, P., Rosenthal, N. A., & Pinto, A. R. (2018). Single-Cell Transcriptional Profiling Reveals Cellular Diversity and Intercommunication in the Mouse Heart. *Cell Reports*, 22(3), 600–610. <https://doi.org/10.1016/j.celrep.2017.12.072>
- van Dam, S., Vösa, U., van der Graaf, A., Franke, L., & de Magalhães, J. P. (2017).

Gene co- expression analysis for functional classification and gene–disease predictions. *Briefings*

in Bioinformatics, bbw139. <https://doi.org/10.1093/bib/bbw139>
Van Deursen, J. M. (2014). The role of senescent cells in ageing. *Nature*, 509(7501),
439–446. <https://doi.org/10.1038/nature13193>

Appendix

Senescent-associated genes retrieved from Senequest (Gorgoulis et al., 2019):

AKR1C2
AKT1
AKT1
ALDH1A3
ALOX15B
ANLN
APLP1
ARG2
ARHGAP19
ATF6
ATM
AURKA
AURKB
BCL2
BCL2L1
BCL2L1
BHLHE40
BIRC5
BLM
BMI1
BMP2
BMP4
BMP7
BRAF
BRAF
BRCA1
BTG2
BUB1
BUB1B
CAMK2B
CAV1
CCDC167
CCL2
CCNA2
CCNB1
CCNB2
CCND1
CCNE1
CD44
CDC20
CDC25C
CDCA2
CDCA3
CDCA5
CDCA8
CDK1
CDK2
CDK4
CDKN1A
CDKN1B
CDKN2A

CDKN2AIP
CDKN2B
CDKN3
CEBPA
CEBPB
CEL
CENPA
CENPN
CENPO
CENPW
CEP55
CGAS
CHEK2
CKAP2L
CKS1B
CSNK2A1
CTNNB1
CXCL8
CXCL8
CXCR2
CYB561A3
DDIAS
DEPDC1
DEPDC1B
DICER1
DKK1
DLGAP5
DNMT1
DPP4
E2F1
E2F1
EBNA1BP2
EDN1
EGFR
EGR1
ELAVL1
EME1
EP300
ERBB2
ERCC6L
ESPL1
ESR1
ETS2
EZH2
FAM83D
FANCD2
FGF2
FGF2
FOXM1
FOXO1
FOXO3
FOXO3
GABPA
GADD45A
GADD45B
GADD45G
GAS2L3
GDF15

GTSE1
HBP1
HDAC1
HIF1A
HJURP
HMGB2
HMMR
HMOX1
HRAS
HSPA1A
ID1
IFNG
IGF1
IGF1
IGF1R
IGFBP2
IGFBP3
IGFBP5
IGFBP7
IL6
ING1
ITGB4
JUN
KAT2B
KAT6A
KDM6B
KIF11
KIF20A
KIF23
KIF2C
KIF4A
KIFC1
KL
KNSTRN
KRAS
LMNA
LMNB1
MAD2L1
MAP3K6
MAPK1
MAPK14
MAPK3
MAPK8
MDM2
MIR22
MIR23A
MKI67
MTOR
MTOR
MXD4
MYBL2
MYC
MYC
NAMPT
NDC80
NEIL3
NEK2
NEK6

NFE2L2
NFKB1
NOS3
NOS3
NOTCH1
NOTCH3
NOX1
NOX4
NRAS
NUDT1
OGG1
OIP5
PBK
PIF1
PIK3CA
PIM1
PIMREG
PIN1
PLA2R1
PLK1
PLK4
PMAIP1
PML
POC1A
PPARGC1A
PPM1D
PRKAA1
PRKAA1
PRKCD
PRODH
PRR11
PSRC1
PTEN
PTEN
PTGS2
PTTG1
PTTG3P
RAC1
RACGAP1
RAD51
RAS
RB1
RBL2
RELA
RPS6KA6
RPS6KB1
RRM2
RSL1D1
SAT1
SDC1
SERPINA4
SERPINE1
SGO1
SHC1
SIRT1
SIRT2
SIRT3
SIRT6

SIRT7
SKA3
SKP2
SMAD3
SMARCB1
SMURF2
SOD2
SOD2
SOX9
SPC24
STAT1
STAT3
STAT5A
STK11
SUV39H1
TACC3
TBX2
TERF2
TERT
TGFB1
THBS1
TICRR
TNF
TNFSF13B
TOP2A
TP53
TP53
TP63
TP73
TPX2
TRIP13
TROAP
TTK
TWIST1
TXNIP
UBE2C
UHRF1
WRN
XRCC5
YAP1
YPEL